

# Photocurrent in nanostructures with asymmetric antidots

M.V. Entin, L.I. Magarill

*Institute of Semiconductor Physics, Siberian Branch of Russian Academy of Sciences, Novosibirsk, 630090, Russia*

The steady current induced by electromagnetic field in a 2D system with asymmetric scatterers is studied. The scatterers are assumed to be oriented cuts with one diffusive and another specular sides. Besides, the existence of isotropic impurity scatterers is assumed. This simple model simulates the lattice of half-disk which have been studied numerically recently. The model allows the exact solution in the framework of the kinetic equation. The static current response in the second order of electric field is obtained. The photogalvanic tensor contains both responses to linear and circular polarization of electromagnetic field. The model possesses non-analyticity with regards to the rate of impurity scattering.

PACS numbers: 73.40.-c, 73.50.Bk, 73.50.Pz

## INTRODUCTION

Nowadays technology allows to fabricate artificial arrays of antidot scatterers which form superlattices in semiconductor heterostructures with a two dimensional electron gas (2DES) (see e.g. [1, 2, 3, 4] and Refs. therein). The size of antidots can be varied from a few microns to a few tens of nanometers at a typical electron density  $n_e \sim 10^{12} \text{ cm}^{-2}$ . Superlattices with circular antidots (disks), known as the Galton board [5], have been realized in experiments [1, 2, 3, 4]. The mathematical theorems of Sinai garanty that the classical dynamics of electrons in such structures is chaotic [6]. The effects of chaotic dynamics and contributions of unstable periodic orbits on electron conductivity have been clearly seen experimentally. They were also analyzed by theoretical methods and numerical simulations in great detail [7]. The irradiation of such superlattices by a microwave field [8] opens interesting possibilities for microwave control of electron current in nanostructures. These systems of relatively large period are classical, and the periodic potential is the source of electron scattering.

Unlike arrays of symmetric antidots, studied experimentally in early works, more sophisticated systems were for a long time out of attention. Meanwhile, systems without inversion symmetry are capable to rectify the electric current. The stationary current in homogeneous media affected by light in the absence of any *dc*-voltage called the *photogalvanic effect* (PGE) was studied since the end of 70th [9, 10, 11, 12, 13, 14]. Similar direct current caused by temporal irreversibility due to simultaneous action of two electromagnetic fields with frequencies  $\omega$  and  $2\omega$  is known as the coherent photogalvanic effect (CPGE) [15].

Appearance of directed transport without obvious directed forces is also known as ratchet effect which has a long history. For example, the behavior of a ratchet under the influence of thermal fluctuations was considered in the textbook by Feynman, Leighton and Sands [16] in connection with the problem of reversibility in statistical mechanics. Recently the ratchet problem attracted a

great interest of the scientific community [17, 18]. In fact the photogalvanic effect corresponds to a ratchet subjected to weak alternating force with zero mean. Such ratchets have been observed in various physical systems including Josephson junction arrays [19, 20, 21], cold atoms [22], macroporous silicon membranes [23], microfluidic channels [24] and other systems. The growing interest to ratchets is strongly stimulated by their possible applications to biological systems [17, 25]. In this sense the artificial asymmetric nanostructures, as those discussed in [26, 27, 28] and here, can serve as a prototype for understanding of photocurrent properties in biomolecules. The results obtained for ratchets induced by microwave fields in nanostructures can be also used for understanding of directed transport created by *ac*-fields in molecular electronics [29].

Relatively recently an artificial lattice of asymmetric antidots (triangles) participating in transport as scatterers of electrons was realized experimentally. It exhibited the direct current induced by alternating electric field [30]. The effect of such type was considered theoretically in [31] by means of the classical kinetic equation for the system with weak asymmetric periodic lateral potential.

Another case of superlattices of asymmetric antidots (semidisks oriented in one direction or the semidisk Galton board) has been proposed and analyzed theoretically [26, 27, 28] by simulations of motion of a particle subjected to alternating force with zero means and collisions with hard-wall antidots. It has been shown that a microwave radiation creates the directed flow of electrons. The velocity of this flow  $v_f$  is proportional to a friction coefficient while the direction of current depends on the microwave polarization. The directed transport induced by a microwave field appears also for an ensemble of noninteracting particles been at a thermal equilibrium at temperature  $T$ . This effect is absent in structures with circular antidots due to symmetry conservation. Recently, semidisk Galton board realized experimentally [32] exhibited the rectification of high-frequency electric field.

In [26, 27, 28] the properties of photocurrent in asym-

metric nanostructures have been explained on the basis of heuristic arguments and extensive numerical simulations. However, the analytical theory of the effect still needs to be developed. This aim is reached in this paper with the help of a kinetic equation approach applied to a specific model of asymmetric scatterers (cuts model). This approach allows to obtain analytical dependence of photocurrent properties on system parameters.

## KINETIC EQUATION APPROACH

Here we study a simple model of anisotropic 2D artificial scatterers, which permits the analytical consideration in the framework of kinetic equation approximation and leads to the PGE. The kinetic equation was used in a number of papers devoted to photogalvanic effect. Unlike the particle dynamics method, this way suggests the developed chaos picture where ergodicity of motion is achieved. At the same time it is free from the voluntary assumptions about the particle friction used in [26, 27].

The system under consideration contains randomly distributed oriented scatterers. The scatterers are assumed to be segments of the length  $D$  oriented along the  $y$  axis; one side (left) of the segment is specular and the other side is diffusive (see Fig. 1). The concentration

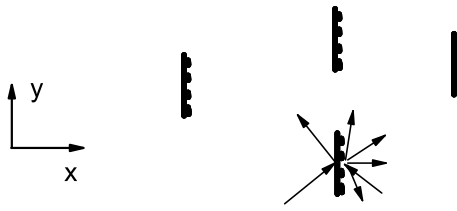


FIG. 1: Considered model system. Cuts have specular left sides and diffusive right sides. This produces anisotropy of scattering resulting in the photocurrent.

of scatterers  $N$  is supposedly low:  $ND^2 \ll 1$ . In this

approximation the kind of spatial distribution of scatterers (random or periodic) is of no importance. Besides, to limit the possible divergency of the result we include isotropic impurity scattering into our model.

This system can be considered as a simplification of the semicircle model studied in [26, 27]. In fact, the diffusive side of the cut scatters particles like round side of the semicircle, if not to pay attention on the difference between randomized (in our case) and deterministic (in semicircle case) motion. The advantage of "cuts" model is its exact solvability.

The kinetic equation reads as

$$\frac{\partial f}{\partial t} + \hat{F}f = \hat{I}f, \quad (1)$$

where  $f(p, \varphi)$  is the distribution function,  $\mathbf{p} = p(\cos \varphi, \sin \varphi)$  is the electron momentum. The term  $(\hat{F}f)$  represents the action of electric field  $\mathbf{E}(t) = \text{Re}(\mathbf{E}_\omega e^{-i\omega t})$  of the electromagnetic wave with the complex amplitude  $\mathbf{E}_\omega = \mathbf{E}_{-\omega}^*$ :

$$\begin{aligned} \hat{F} \equiv \frac{1}{2} \hat{F}_\omega e^{i\omega t} + \text{c.c.} = -e & \left[ E_x \left( \cos \varphi \frac{\partial}{\partial p} - \frac{\sin \varphi}{p} \frac{\partial}{\partial \varphi} \right) + \right. \\ & \left. + E_y \left( \sin \varphi \frac{\partial}{\partial p} + \frac{\cos \varphi}{p} \frac{\partial}{\partial \varphi} \right) \right] \end{aligned} \quad (2)$$

As it will be seen further, the acceleration in the  $y$  direction can not be limited by the scattering on segments only because electrons moving in this direction do not relax. This is why we have not restricted our consideration by the collision with cuts only but have also taken into account the impurity scattering. Hence the collision integral  $\hat{I}f \equiv \hat{I}_i f + \hat{I}_c f$  is assumed to consist of impurity-induced  $\hat{I}_i$  and segment-induced  $\hat{I}_c$  collision integrals. The segment-induced collision integral

$$\hat{I}_c f = \int_0^{2\pi} d\varphi' [W(\varphi', \varphi) f(p, \varphi') - W(\varphi, \varphi') f(p, \varphi)]. \quad (3)$$

is determined by the scattering probability on the cuts  $W(\varphi', \varphi)$ :

$$W(\varphi', \varphi) = \frac{1}{\tau} \left[ \cos \varphi' \theta(\cos \varphi') \delta(\varphi' + \varphi - \pi) - \frac{1}{2} \cos \varphi' \cos \varphi \theta(\cos \varphi) \theta(-\cos \varphi') \right], \quad (4)$$

where  $\tau = (DNv)^{-1}$  is the corresponding characteristic time,  $v = p/m$ ;  $\theta(x)$  is the Heaviside function. The impurity scattering is suggested to be isotropic:

$$\hat{I}_i f = -\frac{1}{\tau_i} (f - \langle f \rangle), \quad (5)$$

where  $\langle \dots \rangle$  means average over angles,  $\tau_i$  is the relaxation time corresponding additional isotropic scattering.

We shall solve the kinetic equation Eq.(1) in the second order on electric field. In the elastic approximation the collision operator is degenerate because its action on

the isotropic function gives zero; thus this operator has an eigenfunction with zero eigenvalue. Physically, this means that the elastic scattering does not change any distribution function depending only on the energy. But if to project the Gilbert space of distribution functions on the subspace with zero angular average, the corresponding projection of the scattering operator becomes non-degenerate. So if to consider only the distribution functions with zero mean, the elastic scattering operator remains non-degenerate and can be treated as full relaxation operator. Inelastic scattering controls only isotropic part of the distribution function which (if it is weaker than elastic one) has no impact on the PGE.

In the second order on alternating electric field the steady current density is described by the phenomenological expression

$$j_i = \alpha_{ijk} E_{\omega,j} E_{-\omega,k}. \quad (6)$$

The symmetry of the considered system allows the following non-zero components of the photogalvanic tensor  $\alpha_{ijk}$ :

$$\alpha_{xxx}, \quad \alpha_{xxy}, \quad \alpha_{yxy} = \alpha_{yyx}^*. \quad (7)$$

From Eq.(6) it follows that components  $\alpha_{xxx}$  and  $\alpha_{xxy}$  are real. The same is valid for all components of  $\alpha_{ijk}$  in the static limit ( $\omega = 0$ ).

The equation (6) is specified as

$$\begin{aligned} j_x &= \alpha_{xxx} |E_x|^2 + \alpha_{xxy} |E_y|^2, \\ j_y &= \text{Re}(\alpha_{yxy})(E_x E_y^* + E_y^* E_x) + \text{Im}(\alpha_{yxy})[\mathbf{E} \mathbf{E}^*]_z. \end{aligned} \quad (8)$$

The components  $\alpha_{xxx}$ ,  $\alpha_{xxy}$  and  $\text{Re}(\alpha_{yxy})$  determine the response to the linear-polarized light. For linear polarization along  $x$  or  $y$  axes the current flows along the  $x$  direction; the current in  $y$  direction appears for tilted linear-polarized electric field. In the case of circular polarization the  $y$  component of the current is determined by  $\text{Im}(\alpha_{yxy})$  (the circular photogalvanic effect) and by the sign of the rotation, while  $x$  component of the current is the sum of responses to  $x$  and  $y$  linear polarized light and does not depend on the sign of  $[\mathbf{E} \mathbf{E}^*]_z$ . Notice that the circular photogalvanic effect vanishes if the frequency  $\omega \rightarrow 0$ .

The formal solution of the Eq.(1) in the second order in electric field is

$$f_2 = \left( \frac{\partial}{\partial t} - \hat{I} \right)^{-1} \hat{F} \left( \frac{\partial}{\partial t} - \hat{I} \right)^{-1} \hat{F} f_0 \quad (9)$$

where  $f_0 = 1/(\exp(\epsilon - \mu)/T)^{-1}$  is the isotropic equilibrium distribution function,  $\mu$  is the chemical potential,  $T$  is the temperature. The kernel of the inverse operator in frequency representation, the Green function  $G^\omega(\varphi', \varphi)$ , satisfies the equation  $(-i\omega + \hat{I})G_\omega(\varphi, \varphi') = \delta(\varphi - \varphi')$ . This equation can be solved exactly:

$$\begin{aligned} G^\omega(\varphi, \varphi') &= -\tau \left\{ \frac{\delta(\varphi - \varphi')}{|\cos \varphi| + \xi} + \frac{|\cos \varphi|}{2} \frac{\cos^2 \varphi' - \xi \cos \varphi' \theta(-\cos \varphi')}{(|\cos \varphi| + \xi)(|\cos \varphi'| + \xi)^2(1 - \Phi(\xi))} + \right. \\ &\quad \left. \frac{\theta(-\cos \varphi)}{(|\cos \varphi| + \xi)^2} \left[ -\cos \varphi \delta(\varphi + \varphi' - \pi) + \xi \cos \varphi \frac{\cos^2 \varphi' - \xi \theta(-\cos \varphi') \cos \varphi'}{2(|\cos \varphi'| + \xi)^2(1 - \Phi(\xi))} \right] \right\} \end{aligned} \quad (10)$$

The operator  $G^\omega$  depends on the frequency via the parameter  $\xi = -i\omega\tau + \tau/\tau_i$ ,

$$\Phi(x) = -\pi x + 2 - \frac{1}{1-x^2} - x^2 \frac{3-2x^2}{1-x^2} \Phi(1, x). \quad (11)$$

The functions  $\Phi(n, \xi)$  denote the integrals expressing via elementary functions:

$$\begin{aligned} \Phi(n, x) &= \int_0^{\pi/2} \frac{dt}{(\cos t + x)^n}, \\ \Phi(1, x) &= -\frac{2}{\sqrt{1-x^2}} \operatorname{arctanh}\left(\frac{-1+x}{\sqrt{1-x^2}}\right). \end{aligned} \quad (12)$$

The stationary part of the correction  $f_2$  can be written

as

$$\bar{f}_2 = \frac{1}{4} G^0 (\hat{F}_\omega G^{-\omega} \hat{F}_{-\omega} + \hat{F}_{-\omega} G^\omega \hat{F}_\omega) f_0; \quad G^0 \equiv G^{\omega=0}. \quad (13)$$

The static current reads

$$j_i = -2e \int \frac{d^2 p}{(2\pi)^2} v_i \bar{f}_2. \quad (14)$$

The photogalvanic tensor is expressed via partial tensor  $\tilde{\alpha}_{ijk}$  for electrons with given  $p$ :

$$\alpha_{ijk} = \frac{e^3}{2m\pi^2} \int_0^\infty dp \tau^2 \left( -\epsilon \frac{\partial f_0}{\partial \epsilon} \right) \tilde{\alpha}_{ijk}. \quad (15)$$

In the degenerate case the partial tensor itself determines the total tensor  $\alpha_{ijk}$ :

$$\alpha_{ijk}(T=0, \epsilon_F) = \alpha_0 \tilde{\alpha}_{ijk}|_{p=p_F}, \quad (16)$$

where  $\alpha_0 = e^3/(4\pi^2 N^2 D^2 v_F)$ ,  $v_F = p_F/m$ ,  $p_F$  is the Fermi momentum,  $\epsilon_F = p_F^2/2m$  is the Fermi energy. At finite temperatures  $T$

$$\alpha_{ijk}(T, \mu) = \int d\epsilon \left( -\frac{\partial f_0}{\partial \epsilon} \right) \alpha_{ijk}(T=0, \epsilon_F = \epsilon). \quad (17)$$

The dimensionless tensor  $\tilde{\alpha}_{ijk}$  can be presented as a function of parameters  $\zeta = \tau/\tau_i$  and  $\xi = \zeta - i\Omega$  ( $\Omega = \omega\tau$ ).

## ANALYTICAL RESULTS

Substituting the stationary part of distribution function (13) into the expression (14) and using the Green function (10) we find after integration:

$$\begin{aligned} \tilde{\alpha}_{xxx}(\xi, \zeta) = & (B(\zeta) - B(\xi)) \left( 1 - \frac{\pi\zeta}{2} + \frac{\zeta^4 + \zeta\xi - 2\zeta^3\xi}{(\xi - \zeta)^2} \Phi(1, \zeta) - \frac{\zeta\xi - 2\zeta\xi^3 + \zeta^4}{(\xi - \zeta)^2} \Phi(1, \xi) + \zeta^2 \frac{\xi^2 - 1}{\xi - \zeta} \Phi(2, \xi) \right) + \\ & B(\zeta) B(\xi) \left( -\frac{\pi\zeta}{2} - \frac{2\zeta(\zeta^4 - \zeta\xi - 3\zeta^3\xi - \zeta^2 + 4\zeta^2\xi^2)}{(\xi - \zeta)^3} \Phi(1, \zeta) + \frac{2\xi(\zeta^4 + \zeta^2(-1 + 4\xi^2) - \zeta(\xi + 3\xi^3))}{(\xi - \zeta)^3} \Phi(1, \xi) - \right. \\ & \left. \frac{\zeta^2(\zeta^3 + \xi - 2\zeta^2\xi)}{(\xi - \zeta)^2} \Phi(2, \zeta) + \frac{\xi^2(\xi - 4\xi^3 + \zeta(-4 + 7\xi^2))}{(\xi - \zeta)^2} \Phi(2, \xi) + \frac{2\xi^3(-1 + \xi^2)}{\xi - \zeta} \Phi(3, \xi) \right) + c.c. \end{aligned} \quad (18)$$

$$\begin{aligned} \tilde{\alpha}_{xyy} = & 1 - 3B(\zeta) + \frac{\pi\zeta(4B(\zeta) - 1)}{2} + (3\zeta^3\xi - \zeta^4 - \zeta\xi + \xi^2 - 2\zeta^2\xi^2 + B(\zeta)(5\zeta^4 + 3\zeta\xi - 15\zeta^3\xi - 3\xi^2 + 10\zeta^2\xi^2)) \frac{\zeta\Phi(1, \zeta)}{(\xi - \zeta)^3} + \\ & + \frac{\xi(\zeta^2 - \zeta\xi - 2\zeta^2\xi^2 + 3\zeta\xi^3 - \zeta^4 + B(\zeta)(3\zeta\xi - 3\zeta^2 + 10\zeta^2\xi^2 - 15\zeta\xi^3 + 5\xi^4))}{(\xi - \zeta)^3} \Phi(1, \xi) + \frac{\zeta^2 B(\zeta)(\zeta^3 + \xi - 2\zeta^2\xi)}{(\xi - \zeta)^2} \Phi(2, \zeta) + \\ & + \frac{\xi^2(\zeta - \xi - \zeta\xi^2 + \xi^3 + B(\zeta)(4\xi - 5\zeta + 8\zeta\xi^2 - 7\xi^3))}{(\xi - \zeta)^2} \Phi(2, \xi) + \frac{2\xi^3 B(\zeta)(\xi^2 - 1)}{\xi - \zeta} \Phi(3, \xi) \end{aligned} \quad (19)$$

$$\begin{aligned} \tilde{\alpha}_{yxy}(\xi, \zeta) = & \left( (\zeta - \xi)(-2\zeta\xi + \pi^2\zeta(\zeta - \xi)(-1 + \xi^2) + \pi(-\xi + \zeta(2 + (\zeta - 3\xi)\xi))) + \xi\Phi(1, \xi)(-(\pi\xi) + \right. \\ & 2\zeta^2(1 + \pi\xi)(-1 + 2\xi^2) + \zeta^3(\pi - 2\pi\xi^2) + 2\zeta\xi(2 + 2\pi\xi - 3\xi^2 - 2\pi\xi^3) + 4\zeta\xi^3(-1 + \xi^2)\Phi(1, \xi)) + \\ & \left. \zeta(\zeta - 2\xi)\Phi(1, \zeta)(-2(-1 + \zeta^2)\xi - \pi(-1 + 2\zeta^2)(-1 + \xi)(1 + \xi) + 2\xi(-\xi^2 + \zeta^2(-1 + 2\xi^2))\Phi(1, \xi)) \right) \times \\ & \left( 2(\zeta - \xi)^2(\pi + \xi - \pi\xi^2 + \xi(-3 + 2\xi^2)\Phi(1, \xi)) \right)^{-1} - \left( \frac{1}{2(\zeta - \xi)^3} \left[ (\zeta - \xi)(-8 + \pi\zeta^3 - 2\zeta^2(1 + \pi\xi) + \zeta\xi(10 + \pi\xi)) - \right. \right. \\ & 2(\zeta^5 + 2\xi - 3\zeta^2\xi - 3\zeta^4\xi + \zeta(2 - 4\xi^2) + \zeta^3(-1 + 6\xi^2))\Phi(1, \zeta) + \\ & \left. \left. 2(-(\xi(-2 + \xi^2)) + \zeta^2\xi(-2 + 3\xi^2) + \zeta(2 - 5\xi^2 + \xi^4))\Phi(1, \xi) \right] \right)^* \end{aligned} \quad (20)$$

The function  $B(\xi)$  is determined by an expression

$$B(\xi) = \frac{1}{2} \frac{(-1 + \xi^2)(-\pi + 2\xi\Phi(1, \xi))}{\pi + \xi - \pi\xi^2 + \Phi(1, \xi)\xi(2\xi^2 - 3)}, \quad (21)$$

The quantity  $\tilde{\alpha}_{xxx}$  has a static ( $\omega \rightarrow 0$ ) limit:

$$\begin{aligned} \tilde{\alpha}_{xxx}(\zeta, \zeta) = & -\zeta B(\zeta)^2 \left( \pi - 8\zeta\Phi(1, \zeta) + 2(-1 + 6\zeta^2) \times \right. \\ & \left. \Phi(2, \zeta) + 4\zeta(1 - 2\zeta^2)\Phi(3, \zeta) + 2\zeta^2(\zeta^2 - 1)\Phi(4, \zeta) \right) \end{aligned} \quad (22)$$

If additionally  $\zeta \rightarrow 0$ ,

$$\tilde{\alpha}_{xxx}(\zeta, \zeta) \approx \frac{1}{6} - \frac{1}{3\pi} \zeta \log(\zeta/2) - \zeta \frac{(4 + 3\pi^2)}{12\pi} + \dots \quad (23)$$

The case of a clean sample gives the limit 1/6. The positive slope of the function  $\tilde{\alpha}_{xxx}(\zeta, \zeta)$  change to negative at very low numerical value of  $\zeta \sim 2 \exp(-1 - 3\pi^2/4)$ . This behavior is plotted on the inset in Fig.2.

If  $\zeta \rightarrow \infty$ ,

$$\tilde{\alpha}_{xxx}(\zeta - i\Omega, \zeta) \approx \frac{\pi}{8\zeta^3} + \dots \quad (24)$$

If the frequency goes to infinity,

$$\begin{aligned} \tilde{\alpha}_{xxx}(\zeta, \zeta + i\Omega) &= \frac{1}{\Omega^2} F(\zeta), \\ F(\zeta) &= \frac{\pi\zeta}{4}, \quad \text{if } \zeta \rightarrow 0, \\ F(\zeta) &= \frac{\pi}{24\zeta}, \quad \text{if } \zeta \rightarrow \infty. \end{aligned} \quad (25)$$

The function  $F(\zeta)$  has the maximum equal to 0.0717 at  $\zeta = 0.455$ . For finite  $\omega$  and  $\zeta \rightarrow 0$   $\tilde{\alpha}_{xxx} \rightarrow 0$ .

The static limit of  $\tilde{\alpha}_{xyy}$  is given by

$$\begin{aligned} \tilde{\alpha}_{xyy}(\zeta, \zeta) = - & \left( 2\pi^2 \zeta (\zeta^2 - 1)^2 + \pi (1 + 2\zeta^4 - 6\zeta^2) + 2 (\zeta + 2\zeta^5 - 2\zeta^3) + \Phi(1, \zeta) (8\zeta^6 - 16\zeta^4 - 6\zeta^3 + 11\zeta^2) + \right. \\ & \left. 4\zeta^3 (2\zeta^4 - 4\zeta^2 + 3) \Phi^2(1, \zeta) \right) \left[ 2 (\zeta^2 - 1) (\pi + \zeta - \pi\zeta^2 + \zeta\Phi(1, \zeta)(2\zeta^2 - 3)) \right]^{-1}. \end{aligned} \quad (26)$$

which yields

$$\tilde{\alpha}_{xyy}(\zeta, \zeta) \approx -\frac{1}{2} + \frac{\zeta}{2\pi} \left( 3 \log \frac{\zeta}{2} + 3 + 2\pi^2 \right) + \dots \quad \text{if } \zeta \rightarrow 0, \quad (27)$$

The function  $\tilde{\alpha}_{xyy}(\zeta, \zeta)$  (similarly to  $\tilde{\alpha}_{xxx}(\zeta, \zeta)$ ) has singularity at  $\zeta = 0$  and changes the sign of slope at very low  $\zeta$ .

For large  $\zeta$  we have

$$\tilde{\alpha}_{xyy}(\zeta + i\Omega, \zeta) \approx -\frac{5\pi}{24\zeta^3} + \dots \quad \text{if } \zeta \rightarrow \infty. \quad (28)$$

If  $\zeta \rightarrow 0$ ,

$$\tilde{\alpha}_{xyy}(\zeta + i\Omega, \zeta) \approx -\pi\zeta \left( \frac{1 + 2\Omega^2}{2\Omega\sqrt{1 + \Omega^2}} - 1 \right). \quad (29)$$

The high-frequency behavior of  $\tilde{\alpha}_{xyy}(\zeta + i\Omega, \zeta)$  is

$$\tilde{\alpha}_{xyy} \approx \frac{\zeta^2(1 - \zeta^2)}{2\Omega^2} \frac{3\pi - 4\zeta - 2\pi^2\zeta - 2\pi\zeta^2 + 2\pi^2\zeta^3 + (8\pi\zeta^2 - \pi + 4\zeta^3 - 8\pi\zeta^4) \Phi(1, \zeta) + 8\zeta^3(\zeta^2 - 1) \Phi^2(1, \zeta)}{\pi(\zeta^2 - 1) - \zeta + \zeta(3 - 2\zeta^2)\Phi(1, \zeta)} \quad (30)$$

with asymptotics

$$\tilde{\alpha}_{xyy} \approx -\frac{\zeta^2}{2\Omega^2} (3 + \log \frac{\zeta}{2}) \dots \quad \text{for } \zeta \ll 1, \quad (31)$$

and

$$\tilde{\alpha}_{xyy} \approx \frac{\pi}{24\zeta\Omega^2} + \dots \quad \text{for } \Omega \gg \zeta \gg 1. \quad (32)$$

In the static limit the component  $\tilde{\alpha}_{xyy}$  can be presented in the form

$$\alpha_{yxy}(\zeta, \zeta) = \frac{1}{6\zeta^2(\zeta^2 - 1)^3} \left( 2(\zeta^2 - 1)(2\zeta^4 - 1 - \zeta^2 + 3\zeta^2\Phi(1, \zeta)) - 3\zeta^2((\zeta^2 - 1)(16\zeta^2 - 11 - 8\zeta^4 + 4\pi\zeta(\zeta^2 - 1)^2) + (15\zeta^2 - 6 - 20\zeta^4 + 8\zeta^6)\Phi(1, \zeta))B(\zeta) \right) \quad (33)$$

For small or large values of  $\zeta$  we have

$$\begin{aligned} \tilde{\alpha}_{yxy}(\zeta, \zeta) &\approx -\frac{1}{3\zeta^2} + \dots \quad \text{if} \quad \zeta \ll 1, \\ \tilde{\alpha}_{yxy}(\zeta, \zeta) &\approx -\frac{\pi}{3\zeta^3} + \dots \quad \text{if} \quad \zeta \gg 1. \end{aligned} \quad (34)$$

For large  $\Omega$

$$\text{Re}(\tilde{\alpha}_{yxy}) \approx \frac{F_1(\zeta)}{\Omega^2}, \quad \text{Im}(\tilde{\alpha}_{yxy}) \approx \frac{F_2(\zeta)}{\Omega^3}, \quad (35)$$

$$\begin{aligned} F_1(\zeta) &= -\frac{1}{4} \left( 20 - 48\zeta^2 + \pi^2(1 - 4\zeta^2) + 6\pi\zeta(-1 + 4\zeta^2) \right. \\ &\quad \left. + 2(26\zeta^2 - 4 - 24\zeta^4 + \pi\zeta(4\zeta^2 - 3))\Phi(1, \zeta) \right), \quad (36) \\ F_2(\zeta) &= \frac{1}{24}(\pi^2(3\zeta - 12\zeta^3) - 96\zeta(\zeta^2 - 4) \\ &\quad + 2\pi(25 - 88\zeta^2 + 24\zeta^4) \\ &\quad - 2\zeta(144 + 9\pi\zeta - 224\zeta^2 - 12\pi\zeta^3 + 48\zeta^4)\Phi(1, \zeta)). \quad (37) \end{aligned}$$

For small and large  $\zeta$  this gives

$$\begin{aligned} \text{Re}(\tilde{\alpha}_{yxy}) &\approx \frac{1}{\Omega^2} \left( -5 - \frac{\pi^2}{4} - 2\ln\left(\frac{\zeta}{2}\right) \right), \quad \text{if} \quad \zeta \rightarrow 0, \\ \text{Re}(\tilde{\alpha}_{yxy}) &\approx -\frac{\pi}{6\Omega^2\zeta}, \quad \text{if} \quad \zeta \rightarrow \infty. \end{aligned} \quad (38)$$

$$\begin{aligned} \text{Im}(\tilde{\alpha}_{yxy}) &\approx \frac{1}{\Omega^3} \left( \frac{25\pi}{12} + \zeta \left( 16 + \frac{\pi^2}{8} + 12\ln\frac{\zeta}{2} \right) \right), \quad \text{if} \quad \zeta \rightarrow 0, \\ \text{Im}(\tilde{\alpha}_{yxy}) &\approx \frac{1}{\Omega^3} \left( \frac{\pi}{12} + \frac{76}{45\zeta} \right), \quad \text{if} \quad \zeta \rightarrow \infty. \end{aligned} \quad (39)$$

## NUMERICAL RESULTS AND DISCUSSION

The Figures 2-5 represent all components of  $\tilde{\alpha}_{ijk}$  calculated according Equations (18-20) at  $T = 0$  versus parameter  $\zeta = \tau/\tau_i$  for different frequencies. These dependencies can be treated as the dependencies of  $\alpha_{ijk}$  on the rate of impurity scattering. The sign of coefficient  $\tilde{\alpha}_{xxx}$  is positive, while the other coefficients change sign. In accord with found asymptotics all components tend to zero for  $\zeta \rightarrow \infty$  and exhibit non-analytical behavior at  $\zeta = 0$ .

Asymptotic behavior  $\tilde{\alpha} \propto \zeta^{-3}$  (or  $\alpha \propto \tau^{-1}$ ) at large  $\zeta$  follows from the odd dependence of the current on the

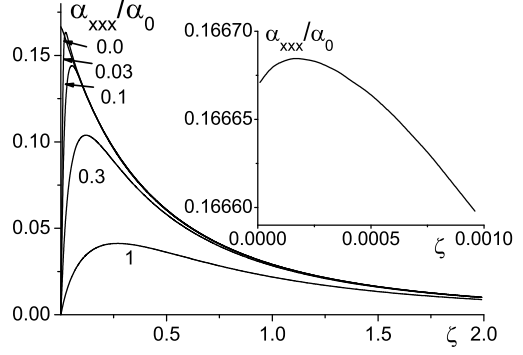


FIG. 2: The dependence of  $\tilde{\alpha}_{xxx}$  on the parameter  $\zeta = \tau/\tau_i$  for different frequencies  $\Omega = \omega\tau = 1, 0.3, 0.1, 0.03, 0$  (marked on curves);  $\alpha_0 = e^3/(4\pi^2 v_F N^2 D^2)$ . Insert: the dependence of  $\tilde{\alpha}_{xxx}$  for small values of the parameter  $\zeta$  at  $\Omega = 0$ .

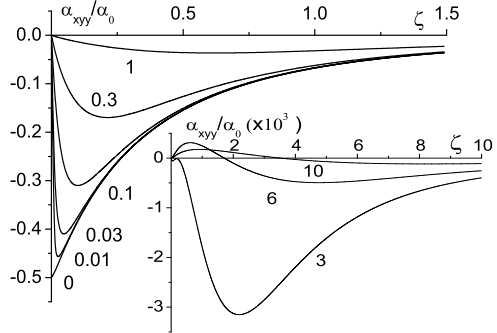


FIG. 3: The dependence of  $\tilde{\alpha}_{yyy}$  on  $\zeta$  for the different parameters  $\Omega$  (marked on curves).

asymmetric scattering on the cuts that results in the proportionality of the current to the scattering rate on cuts for low their concentration. This asymptotics corresponds to case of weak asymmetric scattering usually considered in the theory of PGE.

The value  $\tilde{\alpha}_{ijk}(0, 0)$  depends on the order of limit  $\omega \rightarrow 0, 1/\tau_i \rightarrow 0$ : for example, if first  $\omega \rightarrow 0$  then  $1/\tau_i \rightarrow 0$   $\tilde{\alpha}_{xxx} \rightarrow 1/6$ , else  $\tilde{\alpha}_{xxx} \rightarrow 0$ . Such behavior results from the absence of relaxation of electrons moving

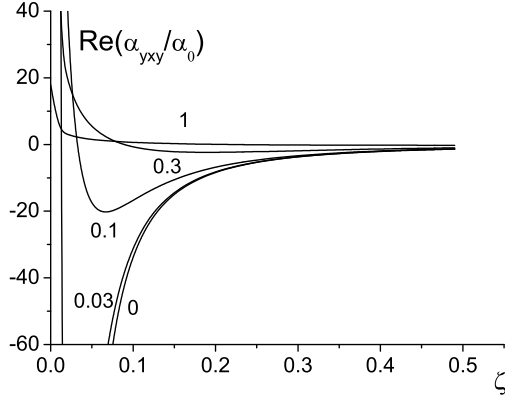


FIG. 4: The dependence of linear photogalvanic coefficient  $\text{Re}(\tilde{\alpha}_{yxy})$  on  $\zeta$  for the same parameters  $\Omega$  as in the Figure 2.

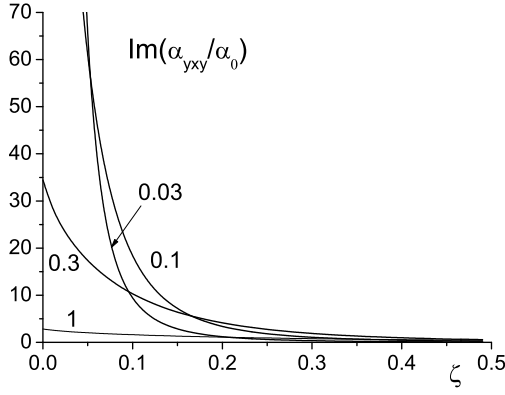


FIG. 5: The dependence of circular photogalvanic coefficient  $\text{Im}(\tilde{\alpha}_{yxy})$  for the same parameters  $\Omega$  as in the Figure 2

along  $y$  axis. The state with  $p_x = 0$  plays role of a drain for electrons. These electrons do not participate in the transport along  $x$  axis, but due to absence of relaxation they accumulate in the state  $p_x = 0$ ; this suppresses the distribution function with finite  $p_x$ , and  $j_x \rightarrow 0$ . On the contrary, the transport along  $y$  axis diverges due to the same reason.

For linear polarized electric field the signs of current components depend on the direction of polarization. Physically, this can be explained by the effective increase of the mean-squared component of electron momentum along field and subsequent increase (decrease) of scattering on the cuts. Let electron with a momentum  $\mathbf{p} = (\pm p, 0)$  impacts with a cut. The change of momentum are equal to  $-2p$  for an electron with the momentum  $\mathbf{p} = (p, 0)$  and  $(1 + 2/\pi)p$  for an electron with the opposite momentum, respectively. In equilibrium this change is compensated by the contributions of other electrons.

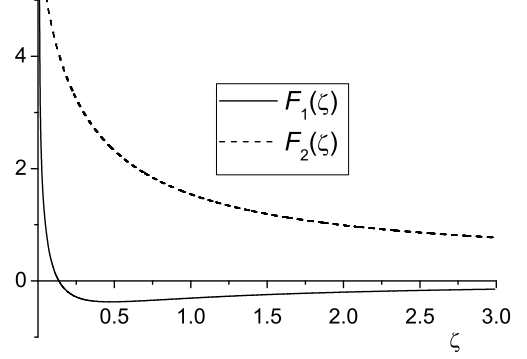


FIG. 6: Asymptotics of photogalvanic coefficient  $\alpha_{yxy} = F_1(\zeta)/\Omega^2 + iF_2(\zeta)/\Omega^3$  for large  $\Omega$ , according to the Equations (36),(37).

But the increase of the mean-squared component of electron momentum along field gives the finite positive contribution to the total current. The acceleration of an electron by the field in  $y$  direction increases  $y$  component of the momentum and produces the opposite direction of  $j_x$ .

The values of coefficients  $\alpha_{yxy}$  are essentially larger than  $\alpha_{xxx}$  and  $\alpha_{xyy}$ . It is a consequence of the fact that the motion along  $y$  direction is collisionless unless the impurity scattering is taken into account. Obviously, the difference is more pronounced at low  $\zeta$ .

It is useful to calculate the possible maximal PGE coefficient. From said above it follows that this maximum is achieved for the component  $\text{Re}(\alpha_{yxy})$  at low frequencies  $\omega \ll 1/\tau_i$  and for clean material  $\tau_i \gg \tau$ . In this case we have

$$j_y = -\frac{1}{48\pi} n_e e v_F \left( \frac{e E l_i}{\epsilon_F} \right)^2 \sin 2\theta, \quad (40)$$

where  $n_e$  is the electron concentration,  $l_i = v_F \tau_i$ ,  $\theta$  is the angle of electric field with respect to the  $x$  direction. The estimation gives the value  $j_y \sim 10^{-5} \text{ A/cm}$  for  $l_i = 10^{-3} \text{ cm}$ ,  $n_i = 10^{12} \text{ cm}^{-2}$ ,  $v_F \sim 10^7 \text{ cm/s}$ .

The special case is the limit of zero impurity concentration. As we have found, in this case for finite frequency the current in  $x$  direction becomes equal to zero and infinity for  $y$  direction. From said above it is evident that the inelastic collisions become essential: they limit this non-analytical behavior. The careful examination of this question is beyond the paper.

The special case is the zero-frequency limit. As we have found, in this case for finite impurity scattering the current in  $x$  direction becomes equal to zero and infinity for  $y$  direction. From said above it is evident that the inelastic collisions become essential: they limit this non-analytical behavior. The careful examination of this question is beyond the paper.

We have restricted ourselves by the classical consideration only. Two quantum factors have not been taken into account: comparability of  $\hbar\omega$  with characteristic electron energies, the Fermi energy and the temperature, and the quantum corrections to conductivity. It should be emphasized that in used approximation the PGE in the metal case does not depend on the temperature in the low temperature limit. This is because the momentum relaxation in metal is temperature-independent (unlike energy relaxation). Despite the involvement of energy relaxation into the control on the distribution function, the current in the second order in electric field is determined by the contributions which do not depend on energy relaxation.

The quantum corrections suppress the low temperature transport and should lead to the temperature dependence of the effect. Both modelling of [26, 27] and the present theory neglect quantum corrections. Thereupon, the temperature dependence of steady current in [26, 27] is not clear. The approach of these papers used a friction force essentially depending on the excess electron energy. Possibly, it is the reason of the temperature dependence. It should be mentioned that the quantum corrections are of less importance in high-mobility samples utilized usually in experiments with antidots.

### COMPARISON WITH NUMERICAL SIMULATIONS

In this section we compare our results with the simulations of the flow velocity of a particle colliding with semidisks.[28] We consider the model used here as a simplification of the semidisks model of Ref. [28]. The essential differences between approaches of Ref.[28] and the present paper are: periodic/random distribution of asymmetric scatterers, deterministic/chaotic character of electron scattering on antidots and motion between them, and absence/presence of the gas approximation. However, the case of low density of semidisks and weak friction corresponds to the gas approximation because the scattering randomizes the motion well enough, and the results of both approaches should be in accord with each other.

The Fig.6 in [28] shows approximate quadratic dependence of the flow velocity on the alternating field what agrees with the second-order in field approximation used in the present paper.

The dependence Fig.7 from [28] demonstrates the drop of the flow velocity with the growth of the semidisk size. This behavior qualitatively corresponds to the drop  $\alpha_{xxx} \rightarrow 0$  for  $\tau \rightarrow 0$  (Fig.2 of present paper). At the same time there is no drop in this figure for large  $\tau \rightarrow \infty$  following from the present paper.

The dependence of the flow velocity on the distance between semidisk centers (Fig.8 from [28]) can be treated

as rescaled dependence of  $\alpha_{xxx}$  on the mean free time  $\tau$  which in the present case vanishes both for  $\tau \rightarrow 0$  and  $\tau \rightarrow \infty$  (Fig.2 of the present paper).

The dependence of the flow velocity (Fig.9 in [28]) on the impurity scattering also has a drop for  $\tau_i \rightarrow 0$ , like expected from the Eq.(24), but there is no drop in this figure for large  $\tau_i$ .

Hence, there is a partial qualitative accordance between the present results and computer simulations of [28]. The origin of discrepancy needs additional study.

### CONCLUSIONS

The considered system of oriented asymmetric scatterers-cuts has  $\alpha_{xxx}$ ,  $\alpha_{xyy}$ , and  $\alpha_{yxy}$  non-zero components of photogalvanic tensor. The linear photogalvanic effect is determined by  $\alpha_{xxx}$ ,  $\alpha_{xyy}$ , and  $\text{Re}(\alpha_{yxy})$ . The circular-polarized illumination, causes the response of the  $y$  component of current only, determined by  $\text{Im}(\alpha_{yxy})$ . The static limit of the current in impurity-free system is ambiguous, depending on value of the product of frequency to the impurity mean-free time. The  $x$  component of the current is limited and in the impurity-free system tends to zero, while the  $y$ -component tends to infinity. This is explained by the accumulation of electrons in the state with zero  $x$ -component of momentum.

The authors are grateful to D.L. Shepelyansky and A.D. Chepelyansky for numerous helpful discussions of the problem. The work was supported by grants of RFBR Nos. 05-02-16939 and 04-02-16398, Program for support of scientific schools of the Russian Federation No. 593.2003.2 and INTAS No. 03-51-6453.

---

- [1] D. Weiss, M. L. Roukes, A. Menschig, P. Grambow, K. von Klitzing, and G. Weimann, Phys. Rev. Lett. **66**, 2790 (1991).
- [2] G.M. Gusev, Z.D.Kvon, V.M.Kudryashov, L.V.Litvin, Y.V.Nastaushev, V.T.Dolgopolov, and A.A.Shashkin, JETP Lett. **54**, 364 (1991) [Pis'ma Zh. Eksp. Teor. Fiz. **54**, 369 (1991)].
- [3] Z.D. Kvon, O. Estibals, A.Y. Plotnikov, J.C. Portal, and A.I. Toropov, Physica E **13**, 752 (2002)
- [4] J. Eroms, M. Tolkiehn, D. Weiss, U. Rössler, J. De Boeck, and G. Borghs, Europhys. Lett. **58**, 569 (2002)
- [5] F. Galton, *Natural inheritance*, (Macmillan, London, 1889).
- [6] I. P. Kornfeld, S. V. Fomin, and Ya. G. Sinai, *Ergodic theory*, (Springer, Berlin, 1982).
- [7] R. Fleischmann, T. Geisel, and R. Ketzmerick, Phys. Rev. Lett. **68**, 1367 (1992); Europhys. Lett. **25**, 219 (1994).
- [8] A.A. Bykov, G.M. Gusev, Z.D.Kvon, V.M.Kudryashov, and V.G.Plyukhin, Pis'ma Zh. Eksp. Teor. Fiz. **53**, 407 (1991) [JETP Lett. **53**, 427 (1991)].

- [9] E.M.Baskin, M.D.Blokh, M.V.Entin, and L.I.Magarill, Phys.Stat.Sol.(b) **83**, K97 (1977).
- [10] E.M.Baskin, L.I.Magarill, and M.V.Entin, Sov.Phys.-Solid State **20**, 1403 (1978).
- [11] V.I.Belinicher, V.K.Malinovskii, and B.I.Sturman, Sov.Phys. - JETP **46**, 362 (1977).
- [12] V.I.Belinicher and B.I.Sturman, Sov. Phys. - Usp. **23**, 199 (1980) [Usp. Fiz. Nauk **130**, 415 (1980)].
- [13] E.L.Ivchenko, G.E.Pikus, in *Semiconductor Physics*, V.M. Tushkevich and V.Ya. Frenkel, Editors, Cons. Bureau, p.427, New York (1986)
- [14] E.L.Ivchenko, G.E.Pikus, *Superlattices and Other Heterostructures*, Springer Series in Solid-State Sciences, v.**110**, 1997.
- [15] E.M.Baskin, M.V. Entin JETP Letters, 1988, **48**, 601 (1988).
- [16] R.P.Feynman, R.B.Leighton, and M.Sands, *The Feynman Lectures on Physics* (Addison-Wesley, Reading, MA, 1966), Vol.**1**, Chap.46.
- [17] R.D. Astumian and P. Hänggi, Physics Today **55** (11), 33 (2002).
- [18] P. Reimann, Phys. Rep. **361**, 57 (2002).
- [19] J.B. Majer, J. Peguiron, M. Grifoni, M. Tusveld, and J.E. Mooij, Phys. Rev. Lett. **90**, 056802 (2003).
- [20] J.E. Villegas, S. Savel'ev, F. Nori, E.M. Gonzalez, J.V. Anguita, R. Garcia, and J.L. Vicent, Science **302**, 1188 (2003).
- [21] A.V. Ustinov, C. Coqui, A. Kemp, Y. Zolotaryuk, and M. Salerno, Phys. Rev. Lett. **93**, 087001 (2004).
- [22] C. Mennerat-Robilliard, D. Lucas, S. Guibal, J. Tabosa, C. Jurczak, J.-Y. Courtois, and G. Grynberg, Phys. Rev. Lett. **82**, 851 (1999).
- [23] S. Matthias and F. Müller, Nature **424**, 53 (2003).
- [24] V. Studer, A. Pepin, Y. Chen, and A. Ajdari, Analyst, **129**, 944 (2004).
- [25] F. Jülicher, A. Ajdari and J. Prost, Rev. Mod. Phys. **69**, 1269 (1997).
- [26] A.D.Chepelianskii, and D.L.Shevelyansky, Phys. Rev. B **71**, 052508 (2005).
- [27] G.Cristadoro, and D.L.Shevelyansky, Phys. Rev. E **71**, 036111 (2005).
- [28] A.D.Chepelianskii, cond-mat/0509679 .
- [29] C. Joachim and M.A. Ratner, PNAS **102** (25), 8801 (2005).
- [30] A.Lorke, S.Wimmer, B.Jager, and J.P.Kotthaus, EP2DS-12, Tokyo, 1997, Conference Workbook, p.105; Physica B **249-251**, 312 (1998). For other examples of ballistic rectifiers see also A. M. Song, A. Lorke, A. Kriele, J. P. Kotthaus, W. Wegscheider, and M. Bichler, Phys. Rev. Lett. **80**, 3831 (1998); S. de Haan, A. Lorke, J.P. Kotthaus, M. Bichler, W. Wegscheider, Physica E, **21**, 916(2004); T.Muller, A.Wurtz, A. Lorke, Appl. Phys. Lett. 87, 042104 (2005).
- [31] L.I.Magarill, Physica E, **9**, 652 (2001).
- [32] Z.D.Kvon, J.Zhang, S.Vitkalov, A.E.Plotnikov, J.C.Portal, A.Wieck (private communication) (2005).